

# Quasi-one-dimensional approximation for Bose-Einstein condensates transversely trapped by a funnel potential

Mateus C. P. dos Santos,<sup>1</sup> Boris A. Malomed,<sup>2,3</sup> and Wesley B. Cardoso<sup>1</sup>

<sup>1</sup>*Instituto de Física, Universidade Federal de Goiás, 74.690-970, Goiânia, Goiás, Brazil*

<sup>2</sup>*Department of Physical Electronics, School of Electrical Engineering,  
Faculty of Engineering, Tel Aviv University, Tel Aviv 69978, Israel*

<sup>3</sup>*ITMO University, St. Petersburg 197101, Russia*

Starting from the standard three-dimensional (3D) Gross-Pitaevskii equation (GPE) and using a variational approximation, we derive an effective one-dimensional nonpolynomial Schrödinger equation (1D-NPSE) governing the axial dynamics of atomic Bose-Einstein condensates (BECs) under the action of a singular but physically relevant *funnel-shaped* transverse trap, i.e., an attractive 2D potential  $\sim -1/r$  (where  $r$  is the radial coordinate in the transverse plane), in combination with the repulsive self-interaction. Wave functions of the trapped BEC are regular, in spite of the potential's singularity. The model applies to a condensate of particles (small molecules) carrying a permanent electric dipole moment in the field of a uniformly charged axial thread, as well as to a quantum gas of magnetic atoms pulled by an axial electric current. By means of numerical simulations, we verify that the effective 1D-NPSE provides accurate static and dynamical results, in comparison to the full 3D GPE, for both repulsive and attractive signs of the intrinsic nonlinearity.

## I. INTRODUCTION

The observation of the Bose-Einstein condensation (BEC) in alkali-metal atomic gas at ultralow temperatures was reported 70 years after it was predicted [1–3]. Currently, BECs are produced and manipulated by various research groups, for various kinds of atomic species [4–6], and are also observed in molecular gases [7, 8]. These settings give rise to countless effects, such as the formation of matter-wave dark [9, 10] and bright [11] solitons, propagation of matter-wave soliton trains [12], creation of vortex states [13, 14], prediction of stable vortex solitons in various forms [15], observation of Feshbach resonances [16], etc. A recent addition to this list is the prediction [17, 18] and experimental creation [19–23] of multidimensional “quantum droplets”, in which the matter-wave collapse is arrested by the Lee-Huang-Yang (LHY) effect, produced by fluctuational corrections to the mean-field dynamics.

The study of static and dynamical properties of dilute BECs at zero temperature is accurately modeled by the time-dependent three-dimensional (3D) Gross-Pitaevskii equation (GPE) [24, 25] (if necessary, complemented by the above-mentioned LHY terms [17, 18]). A relevant problem is to reduce the full three-dimensional GPE to lower-dimensional equations, when the reduction is imposed by an external potential which tightly confines BEC in one or two transverse directions. Several approximations for the dimensional reductions 3D  $\rightarrow$  1D and 3D  $\rightarrow$  2D were elaborated, for both self-repulsive and attractive signs of the nonlinearity in GPE [26–55]. In particular, the use of the variational approximation (VA) for the transverse profile of the wave function, presented in Refs. [27, 28], helps to derive an effective 1D nonpolynomial Schrödinger equation (1D-NPSE), which accurately models the axial dynamics of

the cigar-shaped BECs [56]. This method can also be applied for the derivation of effective 2D-NPSEs, when BEC is strongly confined in the axial direction [27, 45]. This method can be used to analyze the evolution of elongated BECs with [29] or without [30] the assumption that the wave function slowly varies along the axial direction, dynamics of spin-1 condensates [32], and binary self-attractive BECs [33], as well as the behavior of BEC in a nearly-1D cigar-shaped trap with the transverse confining frequency periodically modulated along the axial direction [36, 37, 39, 57], effects of embedded axial vorticity in the elongated BECs [40], matter waves under anisotropic transverse confinement [41], BECs in *funnel-* [42] and tube-shaped [55] potentials, mean-field equations for cigar- and disc-shaped Bose-Fermi mixtures and fermion superfluids [43, 44, 51], solitons and solitary vortices in BECs [45], BECs in mixed dimensions [47], dilute bosonic gases with intrinsic two- and three-body interactions [48], BECs confined in ring-shaped potentials [50], BECs with spin-orbit and Rabi couplings [52–54, 58, 59], etc.

In this work, we consider BEC confined by a *funnel-shaped* potential acting in the transverse plane  $(x, y)$ , i.e., the 2D attractive potential

$$V_{\text{transverse}}(r) = -\frac{\varepsilon^3}{2r}, \quad (1)$$

with  $\varepsilon > 0$  and transverse radial coordinate  $r \equiv \sqrt{x^2 + y^2}$ . As suggested by Ref. [60], this potential may be applied by an axially oriented wire, uniformly charged with density  $\sigma$ , to small molecules carrying a permanent dipole moment  $\mathbf{d}$ , which is oriented along the local electric field, with strength of the radial electric field  $\mathbf{E} = 2\sigma r/r^2$  (the interaction of a neutral polarizable atom with a uniformly charged wire was considered in Ref. [61]). Then, indeed, the potential pulling

the dipoles to the axis is  $V_{\text{transverse}}(r) = -\mathbf{d} \cdot \mathbf{E} \equiv -2\sigma d/r$ , which is tantamount to potential (1). A still more realistic possibility is provided by a quantum gas of atoms carrying permanent magnetic moments (such as chromium, dysprosium, or erbium [4, 62–64]), pulled in the axial direction by an electric-current jet (which may be an electronic beam) [60].

With the help of VA, we derive an effective 1D equation describing the axial dynamics in this setting. A similar configuration was considered in Ref. [42]. However, unlike that work, which used VA based on the Gaussian *ansatz*, we employ one with an exponential profile. This difference is more than a formal modification, as the exponential approximation agrees with the specific asymptotic form of the wave function at  $r \rightarrow 0$ , imposed by the singularity of the funnel trap (see Eq. ((5)) below), while the Gaussian *ansatz* contradicts it. As a result, full 3D numerical simulations demonstrate that we obtain a more accurate model equation for the BEC confined by the funnel-shaped potential (in fact, no solutions of the 1D equation, nor the asymptotic form of the 3D wave function, were considered in Ref. [42]). Limit cases, pertaining to weak- and strong-coupling regimes, are also considered, as well as results provided by the effective equation derived in Ref. [42], for the comparison's sake. Further, we demonstrate that the effective NPSE obtained here also provides an accurate approximation for the transverse width of the confined BEC.

The rest of the paper is organized as follows. In the next section, starting from the 3D GPE and using the VA, we derive an effective NPSE governing the axial dynamics in the funnel-shaped configuration. Limit cases of the NPSE, and a similar effective 1D equation which was derived, in a more formal way, in Ref. [42] are addressed in the same section. Systematic numerical results, for both the static ground states (GSs) and dynamical regimes, are reported in Sec. III. The paper is concluded by Sec. IV.

## II. THE DERIVATION OF THE EFFECTIVE NONPOLYNOMIAL SCHRÖDINGER EQUATION

A monatomic BEC at zero temperature is modeled by the commonly known 3D GPE,

$$i\hbar \frac{\partial \psi}{\partial t} = -\frac{\hbar^2}{2m} \nabla^2 \psi + V(r, z) \psi + \mathcal{N} U |\psi|^2 \psi, \quad (2)$$

where  $\psi(\mathbf{r}, t)$  is the mean-field wave function of the condensate, potential

$$V(r, z) \equiv -\frac{\varepsilon^3}{2r} + V(z) \quad (3)$$

includes the funnel trapping term (1) and a generic (non-singular) axial one,  $V(z)$ ,  $U \equiv 4\pi\hbar^2 a_s/m$  is the nonlinearity strength, with  $a_s > 0$  being the atomic  $s$ -wave

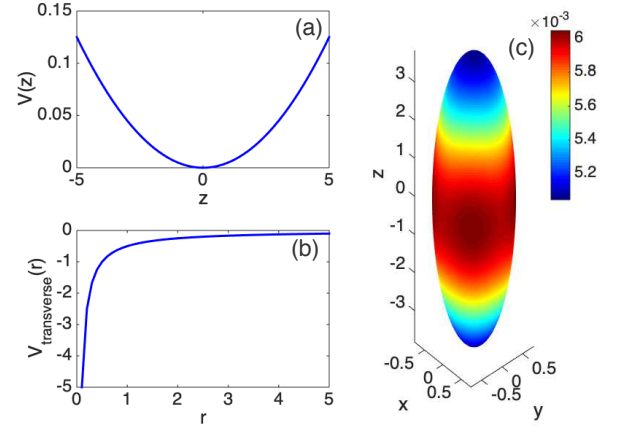


Figure 1. The confining potential, given by Eqs. (3) and (17), in the axial (a) and radial (b) directions. (c) A schematic shape of the density in the respective 3D ground state.

scattering length of repulsive interatomic interactions, and  $\mathcal{N}$  is the number of condensed atoms. By means of rescaling  $t \rightarrow \omega_r t$ ,  $(x, y, z) \rightarrow (x, y, z)/a_r$ ,  $\psi \rightarrow \psi a_r^{3/2}$ , with  $a_r$  being a characteristic length scale in the transverse direction, Eq. (2) is cast in the normalized form,

$$i \frac{\partial \psi}{\partial t} = -\frac{1}{2} \nabla^2 \psi + V(r, z) \psi + 2\pi g |\psi|^2 \psi, \quad (4)$$

with  $g \equiv 2\mathcal{N}a_s/a_r$ .

As concerns the above-mentioned physical interpretation of the model in terms of the condensate of small molecules carrying the permanent electric moment, which are pulled to the uniformly charged axial wire, the respective GPE must take into account the long-range dipole-dipole interaction between the particles. As shown in Ref. [60], this can be done by introducing a mean-field electrostatic field, which is induced by the effective charge density in the dipolar gas (as per the respective Poisson equation),  $\mathbf{E}_d = -4\pi |\psi(x, y, z)|^2 \mathbf{d}$ . This, in turn, gives rise to effective renormalization of the scattering length, which is written in terms of the unscaled notation,  $a_s \rightarrow a_s + md^2/\hbar^2$ . Similarly, the mean-field approximation makes it possible to take into account dipole-dipole interactions between magnetic atoms.

A schematic representation of the trapping potential (3), and expected distribution of the BEC density in the corresponding GS is displayed in Fig. 1. Here, the axial term of the potential,  $V(z)$ , is assumed to take the harmonic-oscillator (HO) form, see Eq. (17) below.

In spite of the presence of the singular potential (1), Eq. (4) gives rise to a GS wave function with chemical

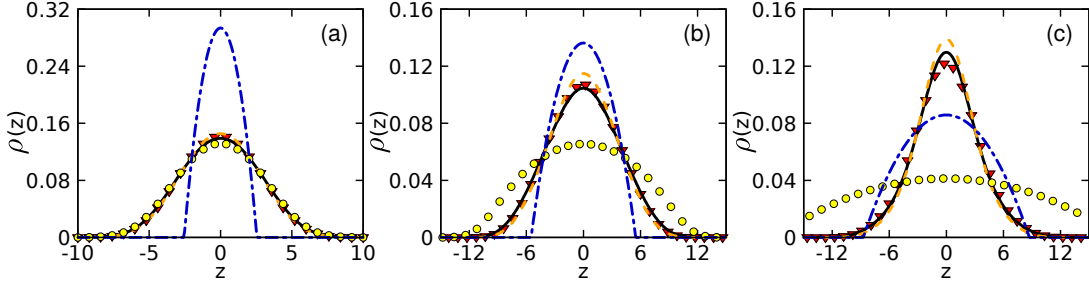


Figure 2. Normalized axial density profiles  $\rho(z)$  for a repulsive BEC ( $g > 0$ ), under the combined action of the funnel trap (1) with  $\varepsilon = 1$  and axial potential (17) with  $\lambda = 0.1$ , for (a)  $g = 1$ , (b)  $g = 10$ , and (c)  $g = 40$ . The density profiles were numerically obtained as GS (ground-state) solutions of the full 3D GPE (4) (red triangles), 1D-NPSE (12) (the black solid line), 1D YXWLH equation (14) (the orange dashed line), cubic 1D-NLSE (15) (yellow circles), and the TF state (16) (the blue dashed-dotted line).

potential  $\mu$  and a regular expansion at  $r \rightarrow 0$ :

$$\psi(r, z, t) = e^{-i\mu t} \left[ \left(1 - \varepsilon^3 r\right) \psi_0(z) + \frac{1}{2} \psi_2(z) r^2 + \dots \right], \quad (5)$$

$$\psi_2(z) = \left( \frac{1}{2} \varepsilon^6 - \mu + V(z) \right) \psi_0(z) + 2\pi g \psi_0^3(z) - \frac{1}{2} \psi_0''(z)$$

[function  $\psi_0(z)$  can be uniquely determined only from the global solution of Eq. (4), rather than solely from the expansion at small  $r$ ]. An essential difference of Eq. (5) from a similar expansion constructed with a nonsingular potential is that, in the latter case, the expansion does not contain a term  $\sim r$ . On the other hand, it is relevant to stress that the GS *does not exist* in the presence of a more singular radial potential, *viz.*,  $V_{\text{transverse}}(r) = -Cr^{-2}$ , with  $C > 0$ . In that case, one can formally find a wave function with a singularity at  $r \rightarrow 0$ ,  $\psi \sim r^{-1}$ ; however, this solution is unphysical, as its norm diverges [60].

The Lagrangian density, corresponding to Eq. (4) with confining potential (3), is

$$\mathcal{L} = \frac{i}{2} \left( \psi^* \frac{\partial \psi}{\partial t} - \psi \frac{\partial \psi^*}{\partial t} \right) - \frac{1}{2} |\nabla \psi|^2 - \left( V(z) - \frac{\varepsilon^3}{2r} \right) |\psi|^2 - \pi g |\psi|^4. \quad (6)$$

Our goal is to reduce the 3D model to an appropriate 1D approximation. To this end, we consider the following factorized *ansatz*:

$$\psi(r, z, t) = \exp\left(-\frac{r}{2\eta^2}\right) \frac{f(z, t)}{\sqrt{2\pi\eta^2}}, \quad (7)$$

where  $f(z, t)$  is an axial wave function, and  $\eta = \eta(z, t)$  is the transverse width, with the normalization condition

$$\int_{-\infty}^{+\infty} |f(z)|^2 dz = 1, \quad (8)$$

which provides unitary normalization of the full 3D wave function (6). Note that the expansion of *ansatz* (7)

at  $r \rightarrow 0$  agrees with the asymptotic form given by Eq. (5).

The effective 1D-NPSE is produced by inserting *ansatz* (7) into Lagrangian density (6) and performing integration in the transverse plane, it being relevant to stress that the 2D integral with singular term  $\sim 1/r$  in Eq. (6) converges. This procedure leads us to the following effective 1D Lagrangian,

$$L_{1D} = \int_{-\infty}^{+\infty} \left[ \frac{i}{2} \left( f^* \frac{\partial f}{\partial t} + \text{c.c.} \right) - \frac{1}{2} \left| \frac{\partial f}{\partial z} \right|^2 - \left[ V(z) + \frac{1}{2\eta^2} \left( \frac{1}{4\eta^2} - \varepsilon^3 \right) \right] |f|^2 - \frac{g}{8} \frac{|f|^4}{\eta^4} \right] dz, \quad (9)$$

where both  $*$  and c.c. stand for the complex conjugation (as usual, the derivation neglects terms including  $\partial\eta/\partial z$ , assuming that the variation of transverse width  $\eta$  follows that of axial density  $|f|^2$  [27, 28]). Euler-Lagrange equations following from the 1D Lagrangian are

$$i \frac{\partial f}{\partial t} = -\frac{1}{2} \frac{\partial^2 f}{\partial z^2} + V(z)f + \frac{1}{2\eta^2} \left( \frac{1}{4\eta^2} - \varepsilon^3 \right) f + \frac{g|f|^2}{4\eta^4} f, \quad (10)$$

$$2\varepsilon^3 \eta^2 - 1 - g|f|^2 = 0. \quad (11)$$

Next, substituting  $\eta^2$  from Eq. (11) in Eq. (10), one arrives at the following time-dependent 1D-NPSE:

$$i \frac{\partial f}{\partial t} = -\frac{1}{2} \frac{\partial^2 f}{\partial z^2} + V(z)f - \frac{\varepsilon^6}{2(1 + g|f|^2)^2} f, \quad (12)$$

which is the main result of the derivation. To test accuracy of the effective 1D-NPSE given by Eq. (12), below we compare it to other approximations.

#### A. The YXWLH equation

An effective 1D equation for BEC under the action of the funnel-shaped potential was proposed in Ref. [42],

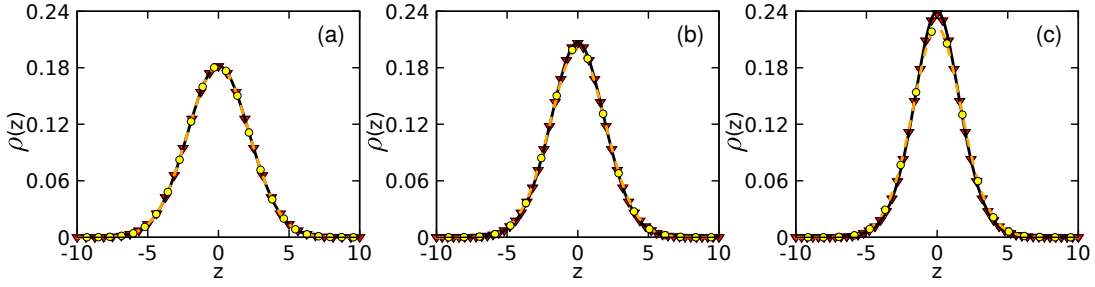


Figure 3. The same as in Fig. (2), but for the self-attractive BEC ( $g < 0$ ), for  $g = -0.05$  (a),  $g = -0.3$  (b), and  $g = -0.5$  (c).

in which the dimensional reduction was performed by means of the VA based on the Gaussian *ansatz* for the transverse wave function:

$$\psi(r, z, t) = \exp\left(-\frac{r^2}{2\eta^2}\right) \frac{f(z, t)}{\sqrt{\pi\delta}}, \quad (13)$$

cf. Eq. (7). The effective 1D equation derived in Ref. [42] is

$$i\frac{\partial f}{\partial t} = -\frac{1}{2}\frac{\partial^2 f}{\partial z^2} + V(z)f - \frac{\pi\epsilon^6}{8(1+g|f|^2)^2}f, \quad (14)$$

which we refer to below as the YXWLH equation. Note that its structure is similar to that of Eq. (12), the difference amounting to replacing coefficient  $1/2$  in front of the nonlinear terms by  $\pi/8 \approx 0.393$ . However, no solutions of Eq. (14) were reported in Ref. [42], and the asymptotic structure of the wave function at  $r \rightarrow 0$  was not considered either, cf. Eq. (5), the latter point being essential in the case of the singular potential.

### B. The weak- and strong-nonlinearity cases

For the weakly interacting BEC, with  $g|f|^2 \ll 1$ , Eq. (12) reduces to the usual 1D nonlinear Schrödinger equation (NLSE) with the cubic term,

$$i\frac{\partial f}{\partial t} = -\frac{1}{2}\frac{\partial^2 f}{\partial z^2} + V(z)f - \epsilon^6 \left(\frac{1}{2} + g|f|^2\right)f. \quad (15)$$

On the other hand, the Thomas-Fermi (TF) approximation, which neglects the spatial derivatives in the GPEs, may be applied in the case of strong self-repulsion. To this end, we substitute a normalized macroscopic wave function,  $\psi(\mathbf{r}, t) = \exp(-r/2 - i\mu t) f/\sqrt{2\pi}$ , in the 3D GPE (note that this expression corresponds to our initial *ansatz* (7) with  $\eta = 1$ ) and perform the integration in the transverse plane,  $(x, y)$ , neglecting, as usual, the kinetic-energy terms, the result being

$$|f(z)|^2 = \begin{cases} \frac{9}{48} [4\mu - 4V(z) + \epsilon^3], & \text{at } \mu + \epsilon^3 > V(z), \\ 0, & \text{at } \mu + \epsilon^3 \leq V(z). \end{cases} \quad (16)$$

In this approximation, chemical potential  $\mu$  is determined by normalization condition (8).

### III. NUMERICAL RESULTS

Numerical results were produced by means of imaginary- and real-time simulations of the full 3D GPE (4), as well as 1D equations (12), (14), and (15). The simulations were performed with the help of the split-step method, that was based on the Crank-Nicolson algorithm. The imaginary-time simulations aimed to produce the system's GS, while the real-time simulations made it possible to explore dynamical behavior of the models.

We start the analysis of trapped states, predicted by the 3D and 1D equations, adopting the HO potential acting in the axial direction,

$$V(z) = \frac{1}{2}\lambda^2 z^2, \quad (17)$$

with  $\lambda^2 \ll 1$ , as the longitudinal potential must be much weaker than its transverse counterpart. To compare the respective GS solutions produced by the 3D and 1D equations, we use the axial-density profile of the 3D state, defined as

$$\rho(z) = \int \int |\psi(x, y, z)|^2 dx dy, \quad (18)$$

while  $\rho(z) = |f(z)|^2$  for the 1D equations. In Fig. 2, we display typical examples of axial densities for repulsive BEC ( $g > 0$ ) in its GS, under the action of the combined potential (3), in which the longitudinal term is given by Eq. (17) with  $\lambda = 0.1$ . These plots demonstrate that the 1D-NPSE provides essentially more accurate results than other approximations, although Eq. (14), being close to the 1D-NPSE, leads to accuracy which is only slightly worse than provided by the main 1D-NPSE approximation. Thus, it is the best approximation in all cases.

Note that, as observed in Fig. 2, the accuracy of the TF approximation improves slowly with the increase of strength  $g$  of the self-repulsion in the underlying GPE (4), while it is usually assumed that the approximation should become better for strong self-repulsion. There are two reasons for that: first, the TF approximation works well with positive confining potentials, such as



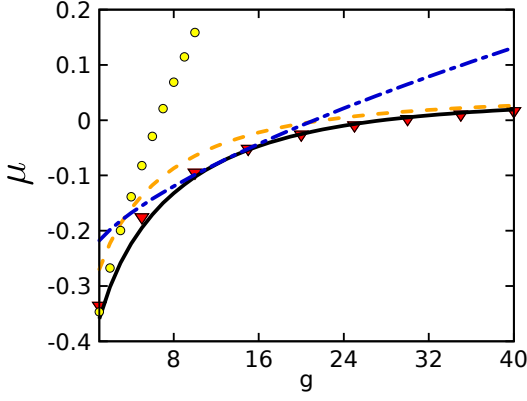


Figure 4. Numerically found chemical potential  $\mu$  of the ground state vs.  $g$  in the self-repulsive BEC ( $g > 0$ ). Parameters and the notation are the same as in Figs. 2 and 3.

the OH trap (17), but not necessarily with the singular negative potential, such as the funnel one in Eq. (3); second, the saturable form of Eq. (12) leads to self-cancellation of the strong nonlinearity.

We also analyzed the case of the self-attractive nonlinearity ( $g < 0$ ), under the action of the same combined potential (3). In Fig. 3, we display GS profiles obtained by means of the imaginary-time propagation, applied to the same set of models, *viz.*, the full 3D GPE, 1D-NPSE, 1D-YWLH equation, and cubic 1D-NLSE, while the TF approximation is not relevant in the case of the self-attraction. In this case, all 1D approximations provide good accuracy in comparison with the full 3D findings.

It is well known that the 3D GPE [65] and its 1D reductions [27, 28] lead to collapse under the action of a sufficiently strong self-attraction. By means of systematic simulations, we have found that the collapse occurs when the attraction strength exceeds a critical value,  $|g| > |g_c|$ , which is  $g_c \simeq -0.9$ ,  $g_c \simeq -0.8$ , and  $g_c \simeq -0.9$ , for the full 3D GPE, 1D-NPSE, and 1D-YXWLH equation, respectively, under the action of the funnel trap (1) with  $\varepsilon = 1$  and longitudinal potential (17) with  $\lambda = 0.1$ . Although the 1D-NPSE model predicts  $g_c$  with a slightly poorer accuracy than the 1D-YXWLH equation (14), the comparison of the 1D profiles of the wave functions (not shown here in detail) demonstrates that the former approximation yields better accuracy at  $|g| \leq 0.8$ .

Getting back to the model with the self-repulsion, in Fig. 4 we display the chemical potential,  $\mu$ , as obtained numerically from the 3D GPE and from 1D approximations for stationary states, which are looked for, respectively, as  $\exp(-i\mu t)\phi(x, y, z)$  or  $\exp(-i\mu t)h(z)$ , with real functions  $\phi$  and  $h$ , cf. Eq. (5). Again, one observes in Fig. 4 that the 1D-NPSE provides very accurate results [in particular, conspicuously more accurate than those produced by the similar 1D-YXWLH approximate equation (14)].

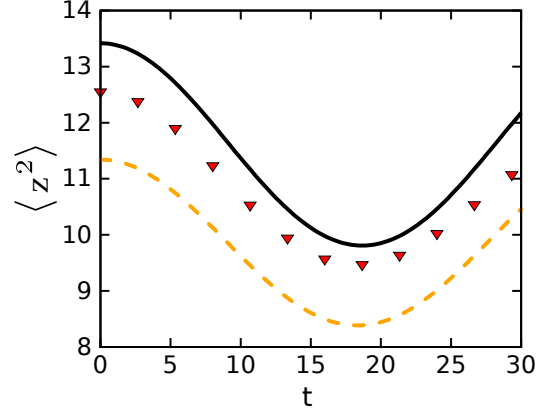


Figure 5. The evolution of the axial mean-squared size  $\langle z^2 \rangle$  of the dynamical state generated by the quench, i.e., sudden perturbation of the ground-state wave function as per Eq. (19). The self-repulsion coefficient is  $g = 5$ , other parameters and the notation being the same as in Figs. 2-4. The results produced by the simplest approximation, in the form of 1D-NLSE (15), are not displayed here, as their difference from the 3D counterparts is very large.

Finally, we check the accuracy of the 1D-NPSE in simulations of dynamical effects. To this end, we used the input in the form of the GS solutions, which were obtained as outlined above, and ran real-time simulations, suddenly replacing longitudinal potential (17) by a slightly stronger one,

$$V(z) \rightarrow 1.2 \times \left( \frac{1}{2} \lambda^2 z^2 \right) \quad (19)$$

(the dynamical behavior of this type is often called *quench* [66]). This variation of the axial confinement gives rise to oscillations of the wave function, which can be observed from the calculation of the axial mean-squared length,  $\langle z^2 \rangle \equiv \int z^2 |\psi(\mathbf{r})|^2 d\mathbf{r}$  for 3D GPE, and  $\langle z^2 \rangle \equiv \int_{-\infty}^{+\infty} z^2 |f|^2 dz$  for the 1D approximations. In Fig. 5 we compare the evolution of  $\langle z^2 \rangle$  as obtained from the simulations of the full 3D GPE and its 1D counterparts. It is again concluded that the 1D-NPSE is more accurate in comparison with the other approximations. Note that the simplest cubic model, based on 1D-NLSE, i.e., Eq. (15), is very inaccurate in the application to dynamical effects, therefore the respective results are not included in Fig. 5.

Lastly, in the case of self-repulsion,  $g > 0$ , Eq. (12) without the axial potential,  $V(z) = 0$ , generates dark solitons. With this form of the saturable nonlinearity, solutions for dark solitons were found in an exact but cumbersome analytical form in Ref. [67]. The comparison of those solutions to their counterparts which may be produced by the 3D equation (2) is a subject for a separate work.

#### IV. CONCLUSION

In this work, by applying the dimensional-reduction method, which is based on the VA (variational approximation), to the full three-dimensional GPE, we have derived an effective 1D-NPSE (nonpolynomial Schrödinger equation with rational nonlinearity) that governs the axial mean-field dynamics of BEC which is tightly trapped in the transverse plane, with both repulsive and attractive signs of the self-interaction. We have considered the specific case when the transverse trapping is imposed by the singular *funnel potential*, which is a singular one,  $\sim -1/r$ . This potential was originally introduced, as a model one, in Ref. [42]. We propose physical settings which give rise to this model, *viz.*, a uniformly charged axial wire attracting particles carrying a permanent dipole electric moment, as well as a bosonic gas of magnetic atoms pulled to the axial electric current. In spite of the singularity, the funnel potential maintains regular wave functions of the trapped states. We verify the accuracy of predictions provided by the 1D-NPSE by comparing them to results of the full 3D simulations, and other 1D approximations, such as the usual cubic one-dimensional NLSE and the Thomas–Fermi approximation. In the case of self-attraction ( $g < 0$ ), the setting gives rise to collapse at  $|g| > |g_c|$ , with the critical value also accurately predicted by the 1D reduction. Finally, the 1D-NPSE also provides a sufficiently accurate approximation for dynamical regimes, initiated by a sudden quench applied to the axial potential. Thus, the approximation based on the 1D equation of the NPSE type is relevant for various types of the transverse trapping potentials, including singular ones, and for the analysis of both the systems’ ground states and dynamical regimes.

Finally, it may be interesting to generalize the above analysis for modes with embedded vorticity  $S = 1, 2, 3, \dots$ , represented by factor  $\exp(iS\theta)$  in the 3D solution, where  $\theta$  is the angular variable in the transverse plane [68]. Then, the expansion similar to that in Eq. (5) starts with terms  $\psi = \exp(-i\mu t + iS\theta) r^S \left\{ \left[ 1 - \varepsilon^3 (1 + 2S)^{-1} r \right] \psi_0(z) + \dots \right\}$ . This extension of the analysis will be reported elsewhere.

#### ACKNOWLEDGMENTS

We appreciate valuable discussions with Luca Salasnich. Financial support from the Brazilian agencies CNPq (#304073/2016-4 & #425718/2018-2), CAPES, and FAPEG (PRONEM #201710267000540 & PRONEX #201710267000503) is acknowledged. This work was performed as part of the Brazilian National Institute of Science and Technology (INCT) for Quantum Informa-

tion (#465469/2014-0). The work B.A.M. is supported, in part, by the joint program in physics between NSF and Binational (US-Israel) Science Foundation through project No. 2015616, by the Israel Science Foundation through Grant No. 1286/17, and by CAPES (Brazil) through program PRINT, grant No. 88887.364746/2019-00.

- 
- [1] M. H. Anderson, J. R. Ensher, M. R. Matthews, C. E. Wieman, and E. A. Cornell, *Science* **269**, 198 (1995).
  - [2] K. B. Davis, M. O. Mewes, M. R. Andrews, N. J. van Druten, D. S. Durfee, D. M. Kurn, and W. Ketterle, *Physical Review Letters* **75**, 3969 (1995).
  - [3] C. C. Bradley, C. A. Sackett, and R. G. Hulet, *Phys. Rev. Lett.* **78**, 985 (1997).
  - [4] A. Griesmaier, J. Werner, S. Hensler, J. Stuhler, and T. Pfau, *Phys. Rev. Lett.* **94**, 160401 (2005).
  - [5] D. G. Fried, T. C. Killian, L. Willmann, D. Landhuis, S. C. Moss, D. Kleppner, and T. J. Greytak, *Physical Review Letters* **81**, 3811 (1998).
  - [6] K. Aikawa, A. Frisch, M. Mark, S. Baier, A. Rietzler, R. Grimm, and F. Ferlaino, *Phys. Rev. Lett.* **108**, 210401 (2012).
  - [7] S. Jochim, M. Bartenstein, A. Altmeyer, G. Hendl, S. Riedl, C. Chin, J. H. Denschlag, and R. Grimm, *Science* **302**, 2101 (2003).
  - [8] M. W. Zwierlein, C. A. Stan, C. H. Schunck, S. M. F. Raupach, S. Gupta, Z. Hadzibabic, and W. Ketterle, *Phys. Rev. Lett.* **91**, 250401 (2003).
  - [9] S. Burger, K. Bongs, S. Dettmer, W. Ertmer, K. Sengstock, A. Sanpera, G. V. Shlyapnikov, and M. Lewenstein, *Physical Review Letters* **83**, 5198 (1999).
  - [10] J. Denschlag, J. E. Simsarian, D. L. Feder, C. W. Clark, L. A. Collins, J. Cubizolles, L. Deng, E. W. Hagley, K. Helmerston, W. P. Reinhardt, S. L. Rolston, B. I. Schneider, and W. D. Phillips, *Science* **287**, 97 (2000).
  - [11] L. Khaykovich, F. Schreck, G. Ferrari, T. Bourdel, J. Cubizolles, L. D. Carr, Y. Castin, and C. Salomon, *Science* **296**, 1290 (2002).
  - [12] K. E. Strecker, G. B. Partridge, A. G. Truscott, and R. G. Hulet, *Nature* **417**, 150 (2002).
  - [13] M. R. Matthews, B. P. Anderson, P. C. Haljan, D. S. Hall, C. E. Wieman, and E. A. Cornell, *Physical Review Letters* **83**, 2498 (1999).
  - [14] K. W. Madison, F. Chevy, W. Wohlleben, and J. Dalibard, *Physical Review Letters* **84**, 806 (2000).
  - [15] B. A. Malomed, (2019), arXiv:1904.12081.
  - [16] S. Inouye, M. R. Andrews, J. Stenger, H.-J. Miesner, D. M. Stamper-Kurn, and W. Ketterle, *Nature* **392**, 151 (1998).
  - [17] D. S. Petrov, *Physical Review Letters* **115**, 155302 (2015).
  - [18] D. S. Petrov and G. E. Astrakharchik, *Physical Review Letters* **117**, 100401 (2016).
  - [19] C. R. Cabrera, L. Tanzi, J. Sanz, B. Naylor, P. Thomas, P. Cheiney, and L. Tarruell, *Science* **359**, 301 (2018).
  - [20] P. Cheiney, C. R. Cabrera, J. Sanz, B. Naylor, L. Tanzi, and L. Tarruell, *Physical Review Letters* **120**, 135301 (2018).
  - [21] G. Semeghini, G. Ferioli, L. Masi, C. Mazzinghi, L. Wolswijk, F. Minardi, M. Modugno, G. Modugno, M. Inguscio, and M. Fattori, *Physical Review Letters* **120**, 235301 (2018).

- (2018).
- [22] G. Ferioli, G. Semeghini, L. Masi, G. Giusti, G. Modugno, M. Inguscio, A. Gallemlé, A. Recati, and M. Fattori, *Physical Review Letters* **122**, 090401 (2019).
  - [23] C. D'Errico, A. Burchianti, M. Prevedelli, L. Salasnich, F. Ancilotto, M. Modugno, F. Minardi, and C. Fort, (2019), [arXiv:1908.00761](#).
  - [24] L. P. Pitaevskii and S. Stringari, *Bose-Einstein Condensation*, International Series of Monographs on Physics (Clarendon Press, 2003).
  - [25] C. J. Pethick and H. Smith, *Bose-Einstein Condensation in Dilute Gases* (Cambridge University Press, Cambridge, 2008).
  - [26] A. Muryshev, G. V. Shlyapnikov, W. Ertmer, K. Sengstock, and M. Lewenstein, *Physical Review Letters* **89**, 110401 (2002).
  - [27] L. Salasnich, A. Parola, and L. Reatto, *Physical Review A* **65**, 043614 (2002).
  - [28] L. Salasnich, A. Parola, and L. Reatto, *Physical Review A* **66**, 043603 (2002).
  - [29] P. Massignan and M. Modugno, *Physical Review A* **67**, 023614 (2003).
  - [30] A. M. Kamchatnov and V. S. Shchesnovich, *Physical Review A* **70**, 023604 (2004).
  - [31] L. D. Carr and J. Brand, *Physical Review Letters* **92**, 040401 (2004).
  - [32] W. Zhang and L. You, *Physical Review A* **71**, 025603 (2005).
  - [33] L. Salasnich and B. A. Malomed, *Physical Review A* **74**, 053610 (2006).
  - [34] W. Matuszewski Michał and Królikowski, M. Trippenbach, Y. S. Kivshar, M. Matuszewski, W. Królikowski, M. Trippenbach, Y. S. Kivshar, W. Matuszewski Michał and Królikowski, M. Trippenbach, and Y. S. Kivshar, *Phys. Rev. A* **73**, 63621 (2006).
  - [35] P. Wei, L. Zhi-Bing, and B. Cheng-Guang, *Chinese Physics Letters* **24**, 2745 (2007).
  - [36] L. Salasnich, A. Cetoli, B. A. Malomed, F. Toigo, and L. Reatto, *Physical Review A* **76**, 013623 (2007).
  - [37] L. Salasnich, A. Cetoli, B. A. Malomed, and F. Toigo, *Physical Review A* **75**, 033622 (2007).
  - [38] A. M. Mateo and V. Delgado, *Physical Review A* **75**, 063610 (2007).
  - [39] A. Maluckov, L. Hadžievski, B. A. Malomed, and L. Salasnich, *Physical Review A* **78**, 013616 (2008).
  - [40] L. Salasnich, B. A. Malomed, and F. Toigo, *Physical Review A* **77**, 035601 (2008).
  - [41] L. Salasnich, *Journal of Physics A: Mathematical and Theoretical* **42**, 335205 (2009).
  - [42] Y. Li, X. Guang-Yuan, W. Yong-Jun, L. Xian-Feng, and H. Jiu-Rong, *Communications in Theoretical Physics* **52**, 431 (2009).
  - [43] C. A. G. Buitrago and S. K. Adhikari, *Journal of Physics B: Atomic, Molecular and Optical Physics* **42**, 215306 (2009).
  - [44] S. K. Adhikari and L. Salasnich, *New Journal of Physics* **11**, 023011 (2009).
  - [45] L. Salasnich and B. A. Malomed, *Physical Review A* **79**, 053620 (2009).
  - [46] A. Muñoz Mateo and V. Delgado, *Annals of Physics* **324**, 709 (2009).
  - [47] L. E. Young-S., L. Salasnich, and S. K. Adhikari, *Physical Review A* **82**, 053601 (2010).
  - [48] W. B. Cardoso, A. T. Avelar, and D. Bazeia, *Physical Review E* **83**, 036604 (2011).
  - [49] A. M. Mateo, V. Delgado, and B. A. Malomed, *Physical Review A* **83**, 053610 (2011).
  - [50] M. Edwards, M. Krygier, H. Seddiqi, B. Benton, and C. W. Clark, *Physical Review E* **86**, 056710 (2012).
  - [51] P. Díaz, D. Laroze, I. Schmidt, and B. A. Malomed, *Journal of Physics B: Atomic, Molecular and Optical Physics* **45**, 145304 (2012).
  - [52] L. Salasnich and B. A. Malomed, *Physical Review A* **87**, 063625 (2013).
  - [53] L. Salasnich, W. B. Cardoso, and B. A. Malomed, *Physical Review A* **90**, 033629 (2014).
  - [54] E. Chiquillo, *Journal of Physics A: Mathematical and Theoretical* **48**, 475001 (2015).
  - [55] M. C. P. dos Santos and W. B. Cardoso, *Phys. Lett. A* **383**, 250401 (2019).
  - [56] J. Cuevas, P. G. Kevrekidis, B. A. Malomed, P. Dyke, and R. G. Hulet, *New Journal of Physics* **15**, 063006 (2013).
  - [57] S. De Nicola, B. A. Malomed, and R. Fedele, *Physics Letters A* **360**, 164 (2006).
  - [58] Y. Li, Z. Luo, Y. Liu, Z. Chen, C. Huang, S. Fu, H. Tan, and B. A. Malomed, *New Journal of Physics* **19**, 113043 (2017).
  - [59] Y. Li, Z. Chen, Z. Luo, C. Huang, H. Tan, W. Pang, and B. A. Malomed, *Physical Review A* **98**, 063602 (2018).
  - [60] H. Sakaguchi and B. A. Malomed, *Physical Review A* **83**, 013607 (2011).
  - [61] J. Denschlag and J. Schmiedmayer, *Europhysics Letters (EPL)* **38**, 405 (1997).
  - [62] I. Ferrier-Barbut, H. Kadau, M. Schmitt, M. Wenzel, and T. Pfau, *Physical Review Letters* **116**, 215301 (2016).
  - [63] M. Schmitt, M. Wenzel, F. Böttcher, I. Ferrier-Barbut, and T. Pfau, *Nature* **539**, 259 (2016).
  - [64] L. Chomaz, S. Baier, D. Petter, M. J. Mark, F. Wächtler, L. Santos, and F. Ferlaino, *Physical Review X* **6**, 041039 (2016).
  - [65] G. Fibich, *The Nonlinear Schrödinger Equation: Singular Solutions and Optical Collapse*, Applied Mathematical Sciences, Vol. 192 (Springer International Publishing, Cham, 2015).
  - [66] J. Dziarmaga, *Advances in Physics* **59**, 1063 (2010).
  - [67] W. Krolikowski and B. Luther-Davies, *Optics Letters* **18**, 188 (1993).
  - [68] L. Salasnich, B. A. Malomed, and F. Toigo, *Physical Review A* **76**, 063614 (2007).